清华大学结构工程与振动教育部重点实验室
陈志鹏　江见鲸　主编

结构工程与振动研究报告集

Research Reports of Structural Engineering and Vibration

7

清华大学出版社

清华大学结构工程与振动教育部重点实验室
陈志鹏　江见鲸　主编

结构工程与振动研究报告集

Research Reports of Structural Engineering and Vibration

7

清华大学出版社
北京

内 容 简 介

本报告集收录清华大学“结构工程与振动教育部重点实验室”研究基金资助课题的论文22篇。内容涉及土木、水利、结构、力学、机械、材料、振动、实验技术等学科，可供上述领域的专业工作人员阅读，也可供高等院校相关专业的师生作为教学或科研的参考资料。

Introduction

The research reports include 22 papers funded by Education Ministry Key Laboratory for Structural Engineering & Vibration of Tsinghua University. It ranges from civil engineering, hydraulic engineering, mechanics, material, mechanical engineering and test technology etc. It is hoped that the reports will serve as a useful reference to professional researchers and college teachers and students in aforementioned fields.

图书在版编目(CIP)数据

结构工程与振动研究报告集. 7/陈志鹏，江见鲸主编. —北京：清华大学出版社，2006.4
ISBN 7-302-10148-5

Ⅰ. 结… Ⅱ. ①陈… ②江… Ⅲ. ①结构工程－研究报告－文集 ②振动－结构工程－研究报告－文集 Ⅳ. TU3-53

中国版本图书馆 CIP 数据核字(2004)第 133537 号

出 版 者：清华大学出版社　　地　　址：北京清华大学学研大厦
　　http://www.tup.com.cn　　邮　　编：100084
　　社 总 机：010-62770175　　客户服务：010-62776969
封面设计：常雪影
印 装 者：清华大学印刷厂
发 行 者：新华书店总店北京发行所
开　　本：185×260　印张：14.5　字数：447 千字
版　　次：2006 年 4 月第 1 版　2006 年 4 月第1 次印刷
书　　号：ISBN 7-302-10148-5/TU · 247
印　　数：1～2000
定　　价：30.00 元

CONTENTS

Seismic Fragility Analysis of Bridges

Howard Hwang[1] *Liu Jingbo*[2]

([1]Center for Earthquake Research and Information, The University of Memphis, Memphis, USA)

([2]Department of Civil Engineering, Tsinghua University, Beijing, China 100084)

Abstract The seismic vulnerability of bridges is usually expressed in the form of fragility curves, which display the conditional probability that the structural demand caused by various levels of ground shaking exceeds the structural capacity defined by a damage state. Fragility curves of structures can be generated empirically and analytically. Empirical fragility curves are usually developed based on the damage reports from past earthquakes, while analytical fragility curves are developed from seismic response analysis of structures and the resulting fragility curves are verified with actual earthquake data, if available. This paper presents an analytical method for the development of fragility curves of highway bridges. In this method, uncertainties in the parameters used in modeling ground motion, site conditions, and bridges are identified and quantified to establish a set of earthquake-site-bridge samples. A nonlinear time history response analysis is performed for each earthquake-site-bridge sample to establish the probabilistic characteristics of structural demand as a function of a ground shaking parameter, for example, spectral acceleration or peak ground acceleration. Furthermore, bridge damage states are defined and the probabilistic characteristics of structural capacity corresponding to each damage state are established. Then, the conditional probabilities that structural demand exceeds structural capacity are computed and the results are displayed as fragility curves. The advantage of this approach is that the assessment of uncertainties in the modeling parameters can be easily verified and refined. To illustrate the proposed method, the method is applied to a continuous concrete bridge commonly found in the highway transportation systems affected by the New Madrid seismic zone in the United States.

Keywords concrete bridge; nonlinear response; seismic vulnerability; uncertainty; fragility curves

1 Introduction

Bridges are one of the most critical components of highway transportation systems. When Bridges are damaged in a seismic event, traffic flows of highway systems may be

interrupted. As a consequence, regional and sometimes even national economics may suffer significant losses. Thus, it is critical to evaluate the seismic vulnerability of highway bridges in earthquake prone regions. The seismic vulnerability of bridges is usually expressed in the form of fragility curves, which display the conditional probability that the structural demand (structural response) caused by various levels of ground shaking exceeds the structural capacity defined by a damage state. Fragility curves of bridges can be developed empirically and analytically. Empirical seismic fragility curves are usually developed based on damage data from past earthquakes (Basoz and Kiremidjian 1998, Shinozuka 2000). On the other hand, analytical seismic fragility curves are developed from seismic response analysis of bridges and the resulting curves are verified with actual earthquake data, if available (Hwang and Huo 1998, Mander and Basoz 1999). This paper presents an analytical approach to develop seismic fragility curves for bridges. To illustrate the proposed method, the method is applied to a continuous concrete bridge commonly found in the highway transportation systems affected by the New Madrid seismic zone in the United States.

2 Seismic fragility analysis procedure

The procedure for the seismic fragility analysis of bridges is as follows:

(1) Select a bridge and establish an appropriate model for the bridge.

(2) Quantify uncertainties in structural parameters used in modeling of bridge and use them to establish a set of bridge samples.

(3) Quantify uncertainties in seismic parameters used in modeling of seismic source and path attenuation. In addition, quantify uncertainties in soil parameters used in modeling of local site condition. On the basis of these seismic and soil random parameters, generate a set of earthquake acceleration time histories, which cover various levels of ground shaking intensity.

(4) Establish a set of earthquake-site-bridge samples from the combination of earthquake samples and bridge samples.

(5) Perform a nonlinear time history response analysis for each earthquake-site-bridge sample to simulate a set of bridge response data.

(6) Perform a regression analysis of simulated response data to establish the probabilistic characteristics of structural demand as a function of a ground shaking parameter, for example, spectral acceleration or peak ground acceleration.

(7) Define bridge damage states and establish the probabilistic characteristics of structural capacity corresponding to each damage state.

(8) Compute the conditional probabilities that structural demand exceeds structural capacity for various levels of ground shaking.

(9) Plot the fragility curves as a function of the selected ground shaking parameter.

3 Bridge model

3.1 Description and modeling of bridge

The bridge selected for this study is a bridge with a continuous concrete deck supported by reinforced concrete column bents. As shown in Fig. 1, the bridge is a four span structure with two 10.0m end spans and two 22.9m interior spans, and thus, the total length of the bridge is 71.8m. The superstructure of the bridge consists of a 17.7m wide, 17.8cm thick, continuous cast-in-place concrete deck supported on 11 AASHTO Type Ⅲ girders spaced at 1.6m (Fig. 2). The girders are supported on reinforced concrete four-column bents. The bearing between the girder and the cap beam of concrete column bent consists of a 2.5cm Neoprene pad and two 2.5cm diameter A307 Swedge dowel bars projecting 22.9cm into the cap beam and 15.2cm up into the bottom of the girder. At the ends of the bridge, the girders are supported on an abutment, which is an integral, open end, spill through abutment with U-shaped wing walls. The back wall is 2.1m in height and 17.7m in width. The wing wall is 2.1m in height and 2.9m in width. The abutment is supported on ten 35.6cm×35.6cm concrete piles.

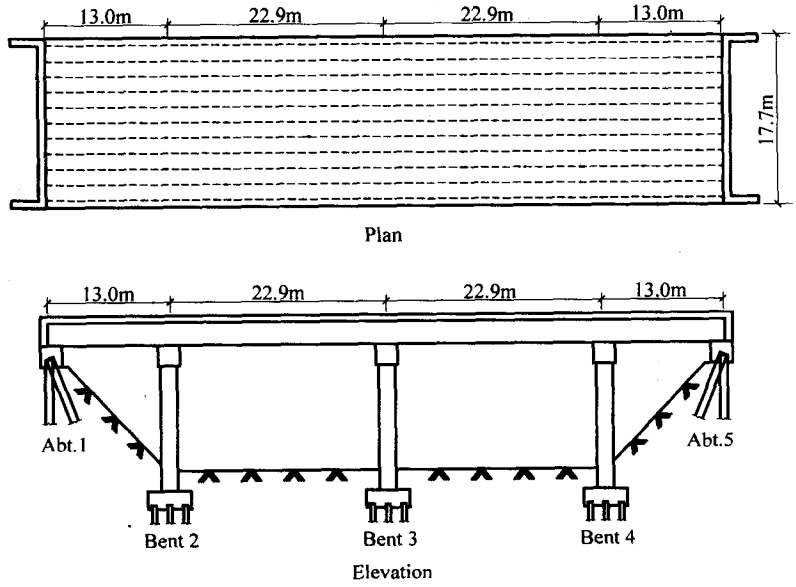

Fig. 1 Plan and elevation of a 602-11 bridge

The concrete column bent consists of a 1.0m by 1.2m cap beam and four 4.6m high, 0.9m diameter columns (Fig. 2). The vertical reinforcing bars of the column consists of 17-# 7 (17φ22), grade 40 vertical bars extending approximately 91.4cm

straight into the cap beam. The vertical bars are spliced at the top of the footing with 17-#7 (17φ22) dowel bars projecting 71.1cm into the column. The dowels have 90-degree turned out from the column centerlines. The column bents are supported on pile footings. The pile cap is 2.7m × 2.7m × 1.1m. The pile cap has a bottom mat of reinforcement consisting of 19-#6 (19φ19) each way located 30.5cm up from the bottom of the pile cap. The pile cap has no shear reinforcement and is supported on eight 35.6cm × 35.6cm precast concrete piles. The piles spaced at 0.8m are reinforced with 4-#7 (4φ22) vertical bars and #2(φ6) square spirals. It is noted that the piles are embedded 30.5cm into the bottom of the pile cap and are not tied to the pile caps with reinforcing bars.

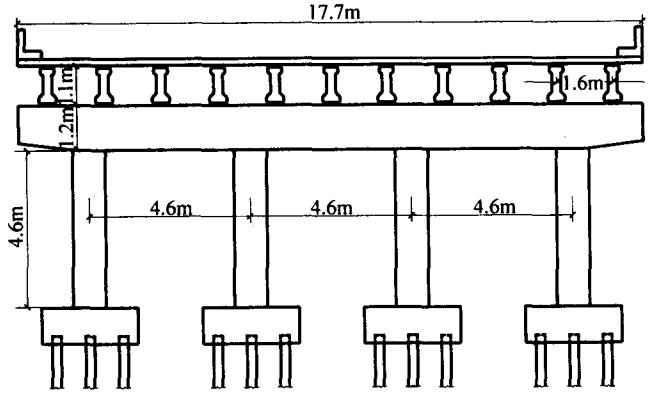

Fig. 2 Transverse section of a 602-11 bridge

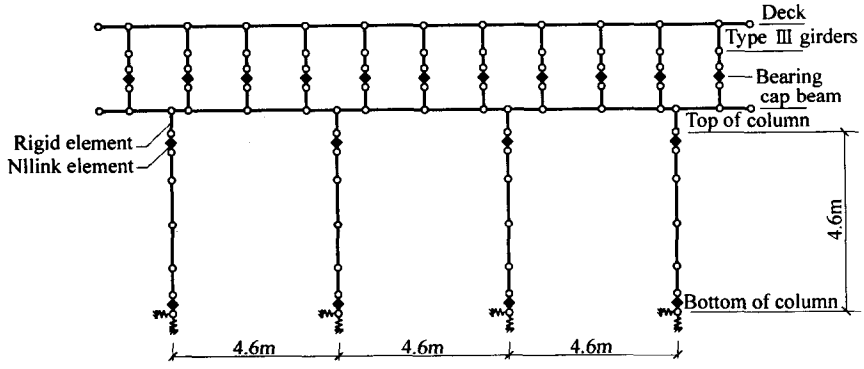

Fig. 3 Transverse view of the bridge finite element model

Several methods are available for modeling of bridge structures (Priestley et al. 1996). In this study, the bridge is modeled with finite elements as described in the computer program SAP2000(1996). A transverse view of the model is shown in Fig. 3. The bridge deck is modeled with 4-node plane shell elements. The girders and cap beams are modeled with beam elements. The bearings between girders and cap beams are modeled using Nllink elements. As shown in Fig. 3, the corresponding nodes between

deck and girder, girder and bearing, bearing and cap beam, and cap beam and top of the column are all connected with rigid elements. Each column is modeled with four beam elements and two Nllink elements placed at the top and the bottom of the column. The bi-linear Nllink element is used to simulate nonlinear column behavior. The pile foundation is modeled as springs. The abutment is modeled using beam elements supported on 11 sub-springs. The detail of bridge modeling is shown in a report by Hwang et al. (2001).

3.2 Uncertainty in bridge modeling

The bridge model includes the bridge structure and supporting springs representing pile footings and abutments. Uncertainties in modeling bridge structure are mainly from uncertainties associated with construction materials, namely, concrete and reinforcement. These uncertainties affect the strength and stiffness of structural members and nonlinear behavior of columns. The uncertainties in supporting springs are mainly from surrounding soils. These uncertainties affect the stiffness of supporting springs.

Following Hwang and Huo(1998), the concrete compressive strength with design value of 20.7MPa is described by a normal distribution with a mean strength of 31.0MPa and a coefficient of variation(COV) of 0.2. The yield strength of grade 40 reinforcement is described by a lognormal distribution with a mean value of 336.5MPa and a COV of 0.11. Ten samples of concrete compressive strength and steel yield strength are generated with each sample in the one-tenth of the probability distributions. These samples are combined using the Latin Hypercube sampling technique to create 10 bridge samples, numbered from bridge sample 1 to bridge sample 10 as shown in Table 1.

Table 1 Material values of ten bridge samples

Bridge sample	Concrete strength and elastic module		Reinforcing steel strength
	f_c(MPa)	E(MPa)	f_y(MPa)
1	26.8	24522	279.2
2	24.6	23473	298.5
3	30.3	26031	339.2
4	20.8	21597	323.2
5	33.4	27361	360.3
6	35.2	28086	310.6
7	31.8	26693	400.9
8	37.4	28968	330.0
9	41.2	30393	349.0
10	28.6	25328	375.0

It is noted that the moment-curvature relation of a column section is derived based on the configuration of column cross section and material strengths as described in the computer program BIAX(Wallace 1992). From this moment-curvature curve, nonlinear characteristics of column sections can be determined and used in the nonlinear seismic response analyses of bridges. Thus, uncertainties in nonlinear behavior of columns are included in the seismic response analysis of bridges.

In this study, spring stiffness of pile footings and abutments is considered to follow a uniform distribution. The mean values are determined as shown in report by Hwang et al. (2001).

Table 2 Stiffness of pile footings

Bridge sample	Lateral stiffness (kN/m)	Torsion stiffness (kN · m/rad)
1	19609	6050
2	21476	6627
3	23344	7203
4	25212	7779
5	29079	8356
6	28947	8931
7	30814	9507
8	32682	10083
9	34549	10660
10	36417	11236

Table 3 Spring stiffness of abutments

Bridge sample	Longitudinal(kN/m)		Transverse(kN/m)	
	Total spring	Sub-spring	Total spring	Sub-spring
1	184243	16749	47826	4348
2	201736	18339	52320	4756
3	219390	19945	56813	5165
4	236883	21535	61468	5588
5	254377	23125	65961	5996
6	272031	24730	70445	6405
7	289524	26320	75109	6828
8	307017	27911	79603	7237
9	324671	29516	84097	7645
10	342165	31106	88751	8068

The coefficient of variation is taken as 30%. Ten samples of spring stiffness are generated according to the specified distribution and assigned to ten bridge samples as listed in Tables 2(pile footings)and 3(abutments).

4 Generation of earthquake acceleration time histories

The process of generating synthetic ground motions is illustrated in Fig. 4. First, a synthetic ground motion at the rock outcrop is generated using a seismological model (Hanks and McGuire 1981, Boore 1983, Hwang and Huo 1994). Then, an acceleration time history at the ground surface is generated from a nonlinear site response analysis. In this study, the first step is performed using the computer program SMSIM(Boore 1996) and the second step is carried out using the computer program SHAKE91(Idriss and Sun 1992). It is noted that the characteristics of seismic source, path attenuation, and local soil conditions are taken into consideration in this process of the generation of synthetic ground motions. The detail of generating synthetic ground motion is described in a report by Hwang et al. (2001).

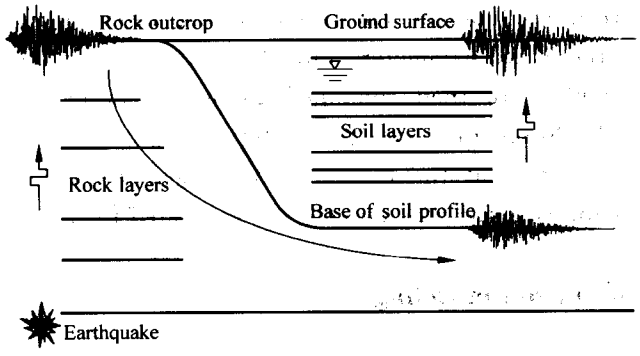

Fig. 4 Illustration of generating synthetic ground motion

4.1 Uncertainty in earthquake modeling

In the generation of earthquake ground motion at the rock outcrop, uncertainties in earthquake source, seismic wave propagation, and rock condition near the ground surface are considered. The seismic parameters, such as the stress parameter $\Delta\sigma$, quality factor Q, and the attenuation parameter κ have significant effects on the resulting ground motion. From a literature review(*Guidelines* 1993, Hwang and Huo 1994), the random seismic parameters are identified and shown in Table 4. These parameters are considered to follow a uniform distribution. In Table 4, the parameter ϕ is the random phase angle, which is used to generate a time series of random band-limited white Gaussian noise. The time at which the peak of the acceleration occurs is also considered as a random variable. It is noted that the strong motion duration T_e is determined from the stress parameter

and other seismic parameters; thus, the duration of ground motion will vary as different values are assigned to these seismic parameters.

Table 4 Uncertainties in seismic parameters

Parameters	Range
Moment magnitude, M	6.0～8.0
Epicentral distance, R	40～100km
Stress parameter, $\Delta\sigma$	100～200bars
Q_0 in quality factor $Q=Q_0 f^\eta$	400～1000
η in quality factor $Q=Q^0 f^\eta$	0.30～0.40
Kappa, κ	0.006～0.01
Focal depth, H	6～15km
Peak parameter, τ_p	0.15～0.3
Phase angle, ϕ	0～2π

For each random seismic parameter listed in Table 4, 100 samples are generated according to its distribution function. The exceptions are the two parameters defining the quality factors. For these two parameters, only 10 samples are established as shown in Table 5. These samples are then combined using the Latin Hypercube sampling technique to establish 100 sets of seismic parameters. For each set of seismic parameters, an acceleration time history at the rock outcrop is generated. Thus, a total of 100 acceleration time histories at the rock outcrop are generated for this study.

4.2 Uncertainties in soil modeling

In this study, the computer program SHAKE91 is used to perform the nonlinear site response analysis. The input soil parameters include the low strain shear modulus, shear modulus reduction curves and damping ratio curves. The uncertainties in these soil parameters are described below.

Table 5 Ten samples of quality factor parameters

Sample	Q_0	η
1	1000	0.30
2	930	0.31
3	870	0.32
4	800	0.33
5	730	0.34
6	680	0.36
7	600	0.37
8	530	0.38
9	470	0.39
10	400	0.40

The low strain shear modulus of soils is estimated using empirical formulas. For sandy soils, the low strain shear modulus is a function of the relative density D_r and for clayey soils, the low strain shear modulus is a function of the undrained shear strength S_u. The ranges of these two soil parameters are taken from hwang and Huo(1994) and listed in Table 6. These two soil parameters are assumed to follow a uniform distribution and 10 samples are generated within the ranges.

Table 6 Uncertainty in soil parameters

Soil classification		Random variable	Range
Sand	Very loose	D_r	0.00～0.15
	Loose		0.15～0.35
	Medium dense		0.35～0.65
	Dense		0.65～0.85
	Very dense		0.85～1.00
Clay	Very soft	S_u	0.00～11.98kN/m^2
	Soft		11.98～23.95kN/m^2
	Medium stiff		23.95～47.90kN/m^2
	Stiff		47.90～95.80kN/m^2
	Very stiff		95.80～191.60kN/m^2
	Hard		191.60～383.20kN/m^2

Uncertainties in the shear modulus reduction curves and damping ratio curves are quantified by an upper bound curve and a lower bound curve. The upper bound curve corresponds to the mean value plus two standard deviations, while the lower bound curve corresponds to the mean value minus two standard deviations(Hwang and Huo 1994). Within the two bound curves, 10 samples are established. As an example, Figs. 5 and 6 show 10 samples of shear modulus reduction curves and corresponding damping ratio curves for clayey soils with PI=15.

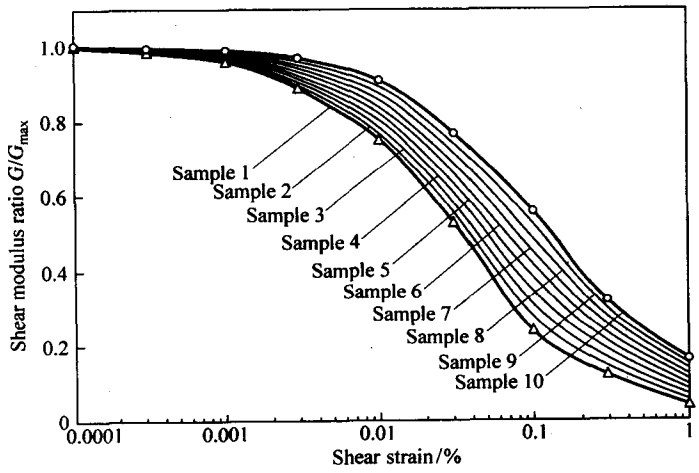

Fig. 5 Ten samples of shear modulus reduction ratio curve for clay with PI=15

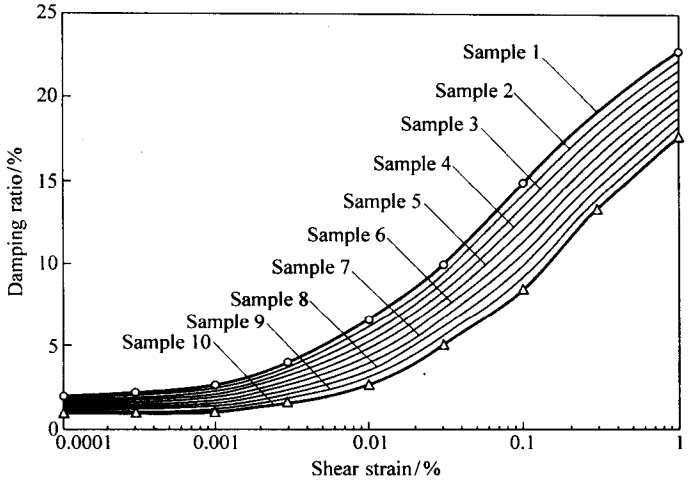

Fig. 6 Ten samples of damping ratio curve for clay with PI=15

The 10 samples of four random soil parameters are used to construct 10 samples of the soil profile, denoted as soil profile 1 to soil profile 10. Each sample of soil profile is matched with 10 earthquake samples to establish 100 earthquake-site samples. For each earthquake-site sample, an acceleration time history at the ground surface is generated from a nonlinear site response analysis using SHAKE91.

4.3 Generation of earthquake-site-bridge samples

In this study, each bridge sample is matched with a soil profile sample, and 10 earthquake samples as illustrated in Fig. 7. Therefore, a total of 100 earthquake-site-bridge samples are established.

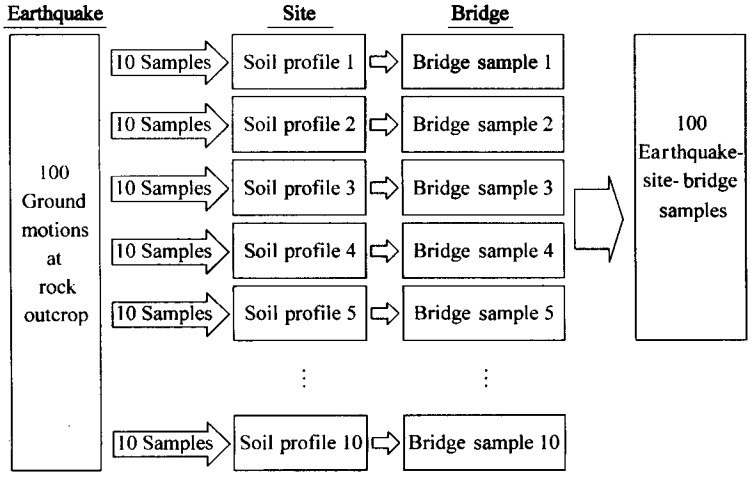

Fig. 7 Generation of earthquake-site-bridge samples

5 Nonlinear seismic response analysis of bridge

The nonlinear seismic response analysis of the bridge is carried out using SAP2000. First, a static analysis of the bridge under dead load is performed, and then a nonlinear time history analysis of the bridge subject to earthquake loading in the transverse direction is carried out. Thus, the response results include both the effects of dead load and earthquake loading. In this study, the acceleration time history is input in the transverse direction. When the bridge is subject to ground motion in the transverse direction, the vibration of the bridge is dominant by the fundamental mode in the transverse direction. As a result, the seismic responses of all columns in all the bents are similar, and the response of any column can be used to represent the response of all the columns.

The bridge used in this study has lap splices at the bottom of the columns; thus, bridge columns are most vulnerable to earthquakes. In this study, damage to a bridge is evaluated using the relative displacement ductility ratio of column, which is defined as

$$\mu_d = \Delta/\Delta_{cyl} \tag{1}$$

where Δ is the relative displacement at the top of a column obtained from seismic response analysis of the bridge, and Δ_{cyl} is the relative displacement of a column when the vertical reinforcing bars at the bottom of the column reaches the first yield.

6 Probabilistic seismic demand and capacity

6.1 Probabilistic seismic demand

For each earthquake-site-bridge sample, a nonlinear time history analysis is carried out using the program SAP2000. The displacement ductility ratios μ_d of column are computed as shown in Figs. 8 and 9 as the function of the spectral acceleration SA and the peak ground acceleration PGA of each input ground motion.

In this study, the probabilistic characteristics of structural demand are described by a lognormal distribution.

$$\mu_d = \ln(\tilde{\mu}_d, \beta_d) \tag{2}$$

where $\tilde{\mu}_d$ is the median value of the structural demand and β_d is the logarithmic standard deviation, which are determined from the regression analysis of the simulated response data. The expression used in the regression analysis is

$$\ln(y) = a + b\ln(x) + \varepsilon \tag{3}$$

where y is the displacement ductility ratio, x is SA or PGA, a and b are the unknown regression coefficients, and ε is a normal random variable with a zero mean and the

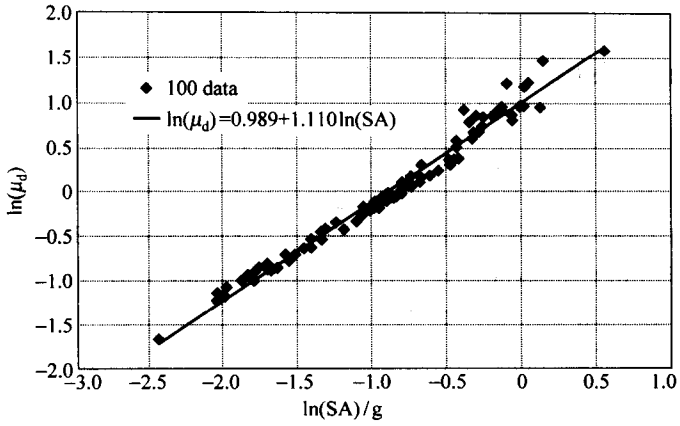

Fig. 8 Regression analysis of displacement ductility ratio versus spectral acceleration

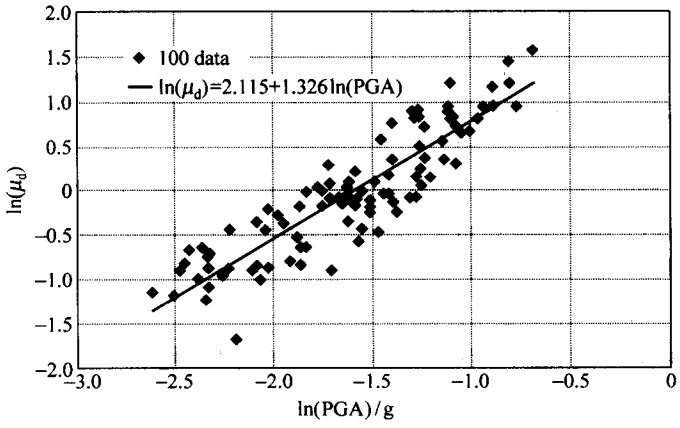

Fig. 9 Regression analysis of displacement ductility ratio versus peak ground acceleration

standard deviation σ to represent the variation of the response data.

From the regression analysis of the response data with respect to SA, the median value of the structural demand is determined as

$$\ln(\tilde{\mu}_d) = 0.989 + 1.110\ln(SA) \tag{4}$$

The standard deviation σ is determined as 0.103. This indicates the regression line fits very well with the response data as shown in Fig. 8.

From the regression analysis of the response data versus PGA, the median value of the structural demand is determined as

$$\ln(\tilde{\mu}_d) = 2.115 + 1.326\ln(PGA) \tag{5}$$

The standard deviation σ is 0.309. This indicates that the displacement ductility ratios are scattered when they are plotted versus PGA as shown in Fig. 9.